

Thermoluminescence dating of heated flint from the Mousterian site of Bérigoule, Murs, Vaucluse, France

D. Richter ^{a,b,g,*}, N. Mercier ^b, H. Valladas ^b, J. Jaubert ^c, P.-J. Texier ^d,
J.-P. Brugal ^e, B. Kervazo ^f, J.-L. Reyss ^b, J.-L. Joron ^b, G.A. Wagner ^a

^a *Forschungsstelle Archäometrie der Heidelberger Akademie der Wissenschaften am Max-Planck-Institut für Kernphysik, Postfach 103980, 69029 Heidelberg, Germany*

^b *Laboratoire des Sciences du Climat et de l'Environnement, UMR CEA-CNRS, Domaine du CNRS, 91198 Gif-sur-Yvette Cedex, France*

^c *Institut de Préhistoire et de Géologie du Quaternaire, Université de Bordeaux I, Avenue des Facultés, 33405 Talence Cedex, France*

^d *CÉPAM, UMR 6130 du CNRS, 250 rue Albert Einstein, 06560 Valbonne, France*

^f *Centre National de Préhistoire, UMR5199-PACEA du CNRS, 38 rue du 26ème R.I., 24000 Périgueux, France*

^e *UMR 6636 du CNRS, MMSH – BP 647, 5 rue du Château de l'Horloge, 13094 Aix-en-Provence, France*

^g *Department of Human Evolution, Max-Planck-Institute for Evolutionary Anthropology, Deutscher Platz 6, 04103 Leipzig, Germany*

Received 9 January 2006; received in revised form 24 May 2006; accepted 13 June 2006

Abstract

The stratigraphic and lithic evidence at the site of Bérigoule is not sufficient for the determination of the age of two Mousterian archaeological layers. Thermoluminescence (TL) dating of heated flint from the two levels provides chronometric age estimates. The TL-ages show a high degree of variability, ranging from 54 to 90 ka for Level I and 67 to 111 ka for Level II. The technological and sedimentological analyses suggest a similar age for the artefacts from the two layers, which is supported by the TL-data. All these data suggest that the artefacts of Levels I and II were heated at the end of OIS 5.

© 2006 Elsevier Ltd. All rights reserved.

Keywords: Thermoluminescence dating; Heated flint; Middle Palaeolithic; Mousterian; Bérigoule; Vaucluse; France

1. Introduction

Typological and technological analysis of lithic assemblages can provide only limited age information. This is especially true for the Middle Palaeolithic period [6] and sites lacking good pedo-sedimentary data and faunal preservation. Due to their variability Mousterian assemblages are difficult to place in a general chronological framework. It is thus necessary to provide archaeology with chronometric dating results, in order to interpret the human occupation in a region. A suite of chronometric dating methods is available to the archaeologist, but often a number of restrictions occur, which

are mainly the lack of availability of suitable material for dating purposes, and/or range limitations of the dating method. On the other hand, material for luminescence dating is, in principle, virtually always available.

2. The Middle Palaeolithic site of Bérigoule

The Middle Palaeolithic site of Bérigoule is located in the region Provence, in the southeast of France (Department of Vaucluse), approximately 45 km east of Avignon (Fig. 1), at an elevation of 560 m a.s.l. The Mont Ventoux and the Nesque Valley to the north, and the mountain ranges of the Luberon and Calavon together with the Basin of Apt to the south and west, frame it, respectively. Climatically, the open-air site is situated in the northern part of the Mediterranean area. It is located at a southern slope running along a fault, which is the northern boundary of a small Oligocene rift. Caves and

* Corresponding author. Department of Human Evolution, Max-Planck-Institute for Evolutionary Anthropology, Deutscher Platz 6, 04103 Leipzig, Germany. Tel.: +49 341 3550354.

E-mail address: drichter@eva.mpg.de (D. Richter).

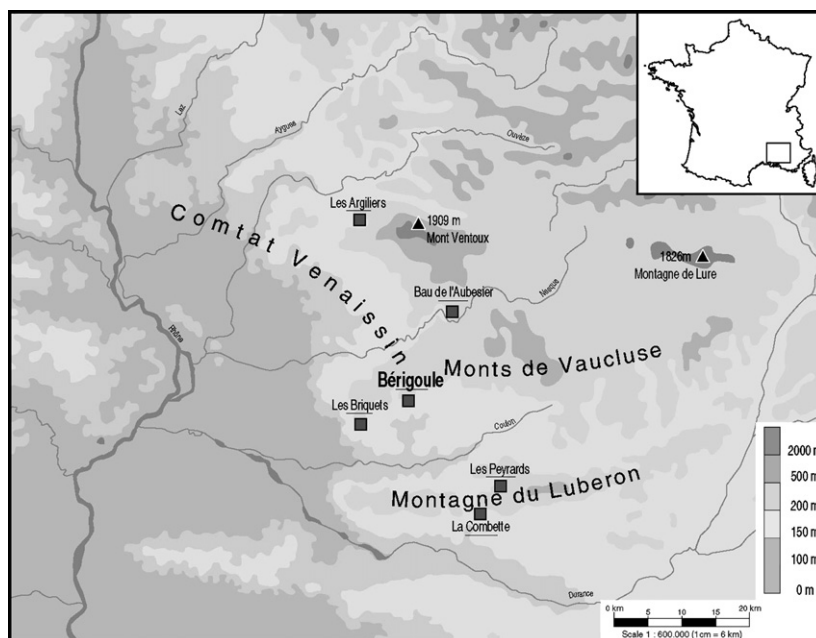


Fig. 1. Location of the Middle Palaeolithic open-air site Bérigoule in southwestern France.

rockshelters are abundant in the area as are flint outcrops (Urgonian facies), one of which is situated at a distance of about 20 m from the site. It is highly likely, that Mousterian people inhabiting the site exploited this outcrop [18]. The region is very rich in Middle Palaeolithic sites, e.g. Bau de l'Aubesier [9], Les Peyrards [10] and La Combette [19]. Bérigoule was discovered in 1988 [3] and excavated by J. Jaubert, P.-J. Texier and J.-P. Brugal between 1988 and 1991 [5].

Two archaeological layers were distinguished in this open-air site, with indications of a third layer in the proximity of the excavated area. The site comprises approximately 150–250 m², of which 45 m² were excavated of the upper level (I), and 10 m² of the lower level (II). A subdivision of the assemblages/layers into distinct occupational levels was possible neither during excavation nor during lithic analysis. The spatial density of flint artefacts was very high, with more than 30,000 pieces larger 3 cm in Level I, but with a much less density in the known part of Level II. This indicates several occupations and suggests the presence of a palimpsest. A large portion of the lithics shows signs of fire damage (30% in Level I).

3. The lithic assemblages

Technologically, Bérigoule is characterized by the omnipresence of Levallois debitage (Fig. 2). Two chaînes opératoires (recurrent unidirectional and centripetal) have been implemented to produce Levallois flakes. For Level I it has been determined that unidirectional and centripetal operative schemes were followed successively or parallel [18].

Level I contains an unusually high proportion of cores (5.2%), of which 62% are classified as Levallois cores (Texier and Jaubert in Ref. [4]). Recurrent unidirectional cores are dominating by 69%, while bipolar cores are rare. Despite

the proximity to the raw material source, many cores were almost completely exhausted. Many of the plain debitage of Levallois flakes had been transformed into retouched tools (>500). The main categories of the tool-kit are: simple scrapers (42.7%), convergent scrapers and Mousterian points or 'déjetés' (32.5%), double scrapers (11.7%), transverse scraper (4.5%), 'dos aminci' (3.7%) and bifacial scrapers (1%). Upper Palaeolithic elements are rare (6%). The large quantity of lithics can be attributed to the proximity of the raw material source. This leads to the interpretation of the function of the site as base settlement [18], which is confirmed by the analysis of the chaîne opératoire. Only few steps/pieces from the chaîne opératoire are missing, indicating that little material was exported. The raw material source was exploited, but the entire processes of tool production and resharpening took place as well in domestic activities.

Typologically, the assemblage can be classified as *Moustérien Ferrassie* in relation to the southwest or north of France, for example, Layer M2 at La Ferrassie, Layers 27, 33, 35, 37 at Combe-Grenal, Chadourne D (Dordogne), Artenac, Lycée Pons (Charente) or Level I at Orgnac 3 (Ardèche). In general, this kind of reduction assigns the assemblage to the beginning of Last Glacial or earlier (Texier and Jaubert unpublished), despite the presence of two Levallois concepts [18].

The lithic assemblage from Level II was obtained from a test pit and is small, with the analysis not completed yet. A preliminary analysis indicates no major differences to the assemblage from Level I. It thus is assigned to the *Moustérien Ferrassie* as well, providing no indications for assessing the difference in time of the production of these two assemblages.

A large portion of artefacts from both layers present a white patina and are partially desilicified [17]. Bones are not preserved, except some thin fragments of teeth and burnt bones from Level II.

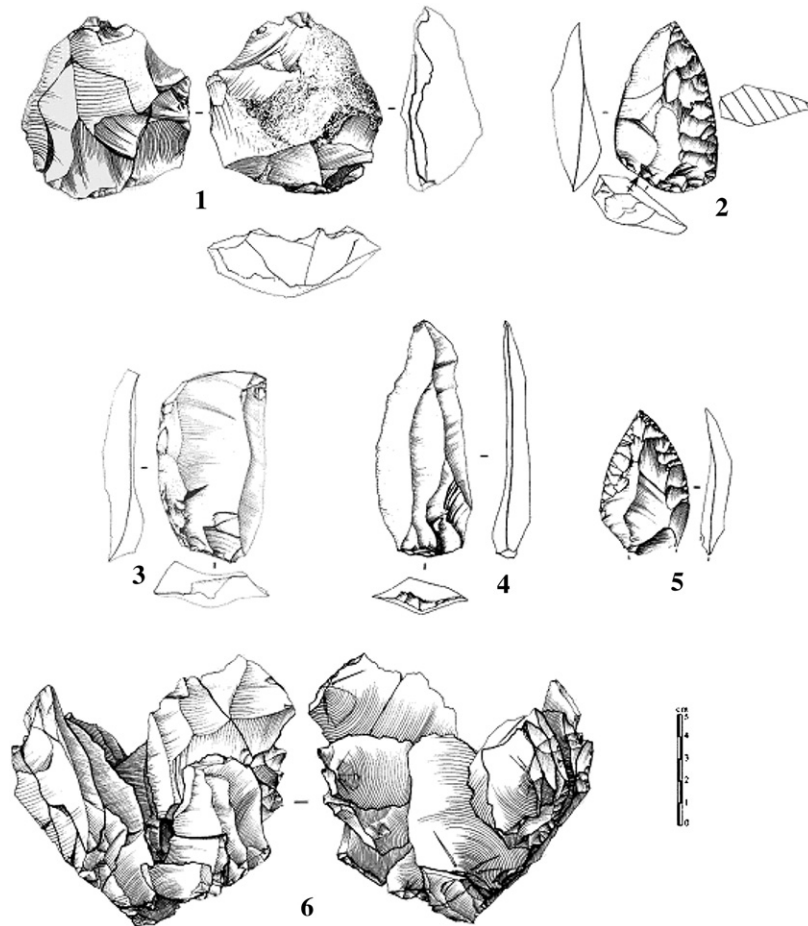


Fig. 2. Examples of the lithic industry at Bérigoule from Level I (1. refitted Levallois flake on a recurrent centripetal core; 2. side scraper with converging heavy retouch; 3. side scraper from a recurrent core; 4. blade from a recurrent unipolar converging core; 5. converging side scraper; 6. refitted centripetal Levallois core, which produced at least five Levallois flakes, of which one was transformed into a side scraper).

4. Stratigraphy

The East–West-profile (Fig. 3) shows a 80-cm thick calcareous slope deposit (A), which is situated below the recent soil. Archaeological Level I is embedded in the clayey deposit B (20–40 cm). A sterile calcareous slope deposit (C) of up to 100 cm thickness follows. The base of the excavated profile, corresponding to layer D, is formed by a brown-red, well-developed clay, in which Level II is situated [18]. Its complete thickness remains undetermined so far, but it amounts to over 70 cm, with the artefacts concentrated in the top portion. Additional stone artefacts were discovered a few metres away from the site, at a level which would correspond to an even older assemblage (Level III, not excavated).

The sedimentological Units A and C are unstructured and characterized by pebbles and cobbles, which are the result of rockfall deposits from upslope rock barriers. The shape of large clasts, the local abundance of angular carbonated granules and sands evidence frost as the responsible agent for the size decrease of the coarse-grained elements. The interstratification of lenses containing gravels and granules also testifies to frequent overland flows.

In Units B and D, the high clay content (40–50%), the decarbonisation and the reddish brown colour of the sediments

indicate well-developed soil forming processes. This might evoke an attribution to OIS 5, but the sharp and sometimes erosive boundaries, the homogeneous composition (clays without gradient) and their massiveness even at the microscopic level shows that the soils were reworked on the slope by mudflows. However, the perturbations had limited consequences, which is indicated by the lack of size sorting of the archaeological material, numerous refittings and the presence of a reddish hearth base in Unit B (Level I).

Consequently, it cannot be determined if the artifacts at Bérigoule have been deposited before, during or after the pedogenesis of these soils.

Because of the abundance of burnt flint in both levels, thermoluminescence techniques appeared to be most suitable for establishing the age of Bérigoule.

5. Thermoluminescence dating of heated flint

The number of burned artefacts in Level I at Bérigoule is unusually high (around 30%). From the vast amount of burnt material from Level I, 11 samples with visible traces of heating (cracks and potlids) were selected. On the basis of the TL-plateau test [1,21], only one sample had to be rejected due to insufficiency of heating in antiquity. The limited excavation of

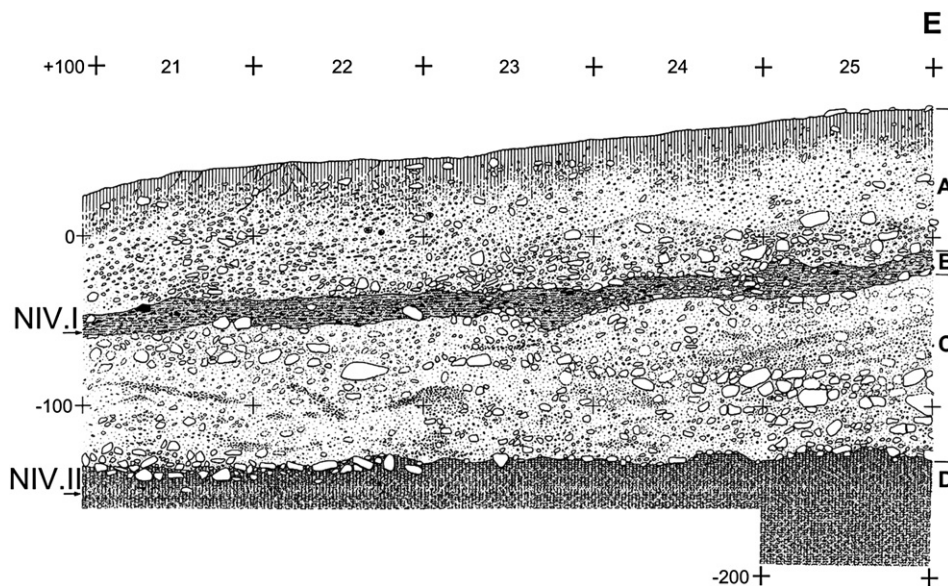


Fig. 3. Bérigoule main profile, east–west: Layer A sterile slope debris. Within the transition to Layer B a few Mousterian artefacts (Level 0) were found. Layer B brown-red clay (Level I, Mousterian). Layer C mostly sterile slope debris. Layer D well developed, thick, brownish-red clay containing Level II (Mousterian). Layer E (not illustrated) sterile slope debris and clay (by J. Jaubert and J.P. Brugal).

Level II of a few square metres provided only six samples, which all were found to be sufficiently burnt for dating.

Luminescence dating requires the determination of the archaeologically acquired radiation dose (palaeodose), as well as dose rates of the internal and external radiation (see for example Ref. [15] for details).

5.1. Dose rate determination

Standard dosimetry methods in the field are usually insensitive to detect temporal variation in the decay chains of radioactive elements. Therefore, sediment samples were taken from the two archaeological layers for analysis in the laboratory. High sensitivity γ - and α -spectrometry on sediment samples from Units B and D revealed that, unlike the Th-series, the U-series decay chain is in disequilibrium (Table 1): such phenomena are accompanied by a partial loss ($\sim 50\%$) of ^{238}U

and ^{234}U but leave ^{230}Th in equilibrium with its daughters (^{214}Bi , ^{210}Pb ; see Table 1). The timing of the uranium loss cannot be determined. Nevertheless, the impact on the final results is limited as the contribution of the U-series to the total annual dose is approximately 30% for each of the two layers. Moreover, the contribution to the total U-series γ -dose rate of the members prior to ^{230}Th to is very small (1.7%). The actual impact on the total dose rate is only a fraction of a percent, and, therefore, has a negligible effect on the resulting dates. However, as these laboratory analyses were performed only on the fine component of the sediment, the results cannot be used as such for the age calculation. All large components of the sediment (artefacts, rocks, etc.), as well as the influence of neighbouring strata have to be taken into account. Therefore, the external γ -dose rates as recorded during one full year by three $\text{CaSO}_4:\text{Dy}$ -dosimeters per level (Table 2) are assumed to be more representative of the different dose rate environments in such sediments, which are described as ‘lumpy’ from a dosimetric perspective [2,16]. For age calculation we used average dosimetric values instead of individual readings

Table 1

Activities (Bq/kg) of some radioisotopes from the uranium and thorium series and potassium content (%) measured by gamma or alpha spectrometry in sediment samples from Bérigoule

Element	Level I	Level II	Method used
U-series	(Bq/kg)	(Bq/kg)	
^{238}U		26.2 ± 2.0	α -spectrometry ^a
^{234}U		24.7 ± 2.5	α -spectrometry ^a
^{230}Th		57.8 ± 2.2	α -spectrometry ^a
^{226}Ra ^b	42.0 ± 0.5	51.3 ± 2.0	γ -spectrometry
Th-series	(Bq/kg)	(Bq/kg)	
^{228}Ac	44.7 ± 0.8	54.5 ± 0.8	γ -spectrometry
^{228}Th	44.8 ± 0.5	54.7 ± 0.7	γ -spectrometry
Potassium	(%)	(%)	
	0.99 ± 0.02	1.37 ± 0.02	γ -spectrometry

^a Average of two subsamples.

^b Measured mainly by ^{214}Bi .

Table 2

Positions and results of CaSO_4 -dosimeters and γ -spectrometry (NaI) in Bérigoule

Dosimeter N°	Square	Level	γ -Dose rate ($\mu\text{Gy/a}$) ^a
D4	S21	I	572
D5	S22	I	563
D6	R20	I	402
NaI-spec.	R21	I	475
D1	S21	II	916
D2	S21	II	930
D3	S22	II	930
NaI-spec.	R21	II	909

^a Corrected for fading, self-dose, cosmic dose, attenuation in case of dosimeters and all with an additional 10% water content. Statistical error $\pm 3\%$.

Table 3
Analytical (NAA) and dose rate data for samples from Bérigoule

Lab. N°.	Square	Level	Element concentrations			Alpha sensitivity	Internal dose rates		External dose rates	
			U ^a (μg/g)	Th ^a (μg/g)	K ^a (wt%)	S _α (μGy/ a/10 ³ α/cm ²)	α-Dose rate (μGy/a)	β-Dose rate (μGy/a)	γ-Dose rate ^b (μGy/a)	Cosmic dose rate (μGy/a)
7	S20	I	0.567	0.106	0.042	25 ± 1	255 ± 25	119 ± 9	482	180
8	R20	I	0.633	0.115	0.017	26 ± 1	289 ± 30	109 ± 9	476	180
10	S20	I	0.712	0.114	0.022	46 ± 1	584 ± 57	124 ± 11	482	180
12	S20	I	0.690	0.114	0.021	20 ± 1	240 ± 23	120 ± 10	492	180
13	S20	I	0.849	0.164	0.035	24 ± 1	357 ± 35	156 ± 13	476	180
14	S20	I	1.587	0.123	0.028	23 ± 1	627 ± 62	257 ± 23	476	180
15	S20	I	1.097	0.124	0.028	16 ± 1	299 ± 30	185 ± 16	487	180
16	S20	I	1.157	0.095	0.017	14 ± 1	287 ± 28	185 ± 17	492	180
17	S20	I	0.769	0.042	0.010	14 ± 1	189 ± 19	121 ± 11	466	180
18	S20	I	0.981	0.205	0.039	18 ± 1	321 ± 30	179 ± 15	492	180
19	S25	II	0.688	0.057	0.012	11 ± 1	130 ± 13	111 ± 10	879	160
20	S22	II	1.267	0.134	0.025	26 ± 1	569 ± 58	208 ± 19	852	160
21	S22	II	1.763	0.052	0.013	22 ± 1	654 ± 66	269 ± 26	861	160
22	S22	II	0.922	0.167	0.029	21 ± 1	342 ± 34	162 ± 14	852	160
23	S25	II	0.968	0.199	0.034	19 ± 1	335 ± 39	173 ± 14	861	160
24	S22	II	0.952	0.189	0.027	18 ± 1	310 ± 30	165 ± 14	879	160

^a A flat error estimate of 10% was applied [8].

^b Corrected for shape and sample mass.

of dosimeters closest to each sample. The distances between dosimeters and samples varied between 0.2 and 2.0 m. In order to adjust for the water loss due to the opening of the sediment by excavation, an increased moisture content of 10% is assumed, which leads to a reduced γ-dose rate of 512 μGy/a for Level I and 925 μGy/a for Level II on basis of the averaged CaSO₄:Dy results (Table 2). In situ measurements with a portable γ-NaI-spectrometer gave similar results (Table 2).

The cosmic dose rate, which depends on the sediment located above the samples, has to be added to the total external dose rate, which is 180 μGy/a for Level I and 160 μGy/a for Level II (Table 3) after Prescott and Hutton [13] for the

respective thickness. An error term of 10% of the total external dose rate was employed in order to take any further unknown/undetected variation of the external dose rate into account.

The internal dose rates were determined by radioactive element analysis with neutron activation analysis (NAA) on material from the fraction < 160 μm [8]. Although all samples are likely to originate from the same source, the variability of element concentrations is large. The radioactive elements of concern in luminescence dating, U, Th and K, vary by a factor of up to five (Table 3). This is reflected by the vastly different internal dose rates, given in Table 4, ranging from 246 to 937 μGy/a.

Table 4
Summarized dose rate data and dating results for Bérigoule

Lab. N°.	BER-	Level	Total internal dose rate ^a (μGy/a)	Total external dose rate ^b (μGy/a)	Total dose rate ^c (μGy/a)	External dose rate ^d (% total dose rate)	Palaeodose (Gy)	Age (ka)
7		I	378 ± 26	662 ± 51	1040 ± 57	64	86.7 ± 7.2	83.4 ± 8.1
8		I	403 ± 31	656 ± 50	1060 ± 59	62	84.6 ± 3.3	79.8 ± 6.5
10		I	714 ± 58	662 ± 51	1376 ± 77	48	74.9 ± 3.2	54.4 ± 4.7
12		I	364 ± 25	672 ± 52	1036 ± 58	65	75.8 ± 3.4	73.2 ± 6.0
13		I	521 ± 38	656 ± 50	1177 ± 63	56	84.3 ± 7.0	71.6 ± 6.8
14		I	897 ± 66	656 ± 50	1554 ± 83	42	93.0 ± 3.0	59.9 ± 4.9
15		I	492 ± 34	667 ± 51	1158 ± 62	58	91.2 ± 4.2	78.7 ± 6.4
16		I	477 ± 33	672 ± 52	1149 ± 61	58	91.3 ± 4.3	79.4 ± 6.5
17		I	319 ± 22	646 ± 49	965 ± 54	67	86.6 ± 4.9	89.8 ± 7.8
18		I	505 ± 34	672 ± 52	1177 ± 62	57	94.0 ± 4.8	79.9 ± 6.6
19		II	246 ± 16	1039 ± 85	1285 ± 87	81	142.7 ± 7.8	111.0 ± 11.1
20		II	789 ± 61	1012 ± 83	1801 ± 102	56	125.9 ± 6.3	69.9 ± 6.3
21		II	937 ± 71	1021 ± 84	1958 ± 110	52	171.6 ± 14.7	87.6 ± 8.6
22		II	513 ± 37	1012 ± 83	1525 ± 90	66	116.5 ± 11.5	76.4 ± 8.6
23		II	518 ± 41	1021 ± 84	1539 ± 93	66	110.9 ± 4.8	72.1 ± 6.4
24		II	482 ± 33	1039 ± 85	1521 ± 91	68	102.6 ± 5.3	67.4 ± 6.1

^a Sum of α- and β-dose rates, plus a minor internal γ contribution.

^b Sum of gamma and cosmic dose rates.

^c Sum of total internal and total external dose rates.

^d External dose rate expressed as percentage of the total dose rate.

5.2. Flint thermoluminescence

The sample preparation and dating procedure as described by Valladas [22] was employed. The inner cores of the flint samples, which had not been exposed to α - and β -radiation from the surrounding sediment, were extracted with a water-cooled diamond saw. After such a removal of the outer 2 mm, the samples were carefully crushed and the resulting 100–160 μm fraction treated with 1 N HCl [22]. Three additive doses were given to natural material with a calibrated ^{137}Cs -source [20] in order to establish the first glow curve for the determination of the equivalent dose. The same total number of four dose points was used for the second glow curve for supralinearity correction on material, of which the TL was zeroed at 350 °C for 90 min, prior to HCl treatment [12]. For TL detection a heating rate of at 5 °C/s was used with an automated TL-reader [24], which is equipped with a Thorn EMI 9635QB photomultiplier. The detection was limited to UV-blue wavelengths by employing glass filters (M.T.O. 397a or 380b). The natural TL ($I_{\text{TL}(n)}$) and the additive TL ($I_{\text{TL}(n+\gamma)}$) for sample BER-13 are shown as an example (Fig. 4A), together with the ratio of natural to additive TL

($I_{\text{TL}(n)}/I_{\text{TL}(n+\gamma)}$), which indicates a wide heating plateau around the peak temperature. The integrated luminescence of the signal within 30 °C above and below the peak temperature (~ 380 °C) was used for the determination of the palaeodose, which was calculated as the sum of equivalent dose and supralinearity correction [1]. These integrals are identical or very similar to the extent of the heating plateaus, and no significant differences were found between the analysis of heating plateau-, ED-Plateau- and the fixed 60 °C-integrals. Data analysis followed Aitken [1] for all samples, which results in different ages than the preliminary published ones [7,14], where some samples were analyzed using an inappropriate slide method. The dose curves for sample BER-13 are demonstrated in Fig. 4B. The resulting palaeodoses show a small dispersion for Level I, but a very large variability for Level II (Table 4). This is – at least for Level II – in concordance with the high variation of radioactive element concentrations and resulting spread of internal dose rates (see above).

The material $< 90 \mu\text{m}$ was crushed further, heated to 500 °C for 10 min and washed with 1 N HCl before deposition on discs following Zimmerman [26]. The sensitivity to α -radiation was then determined by the ratio of normalised

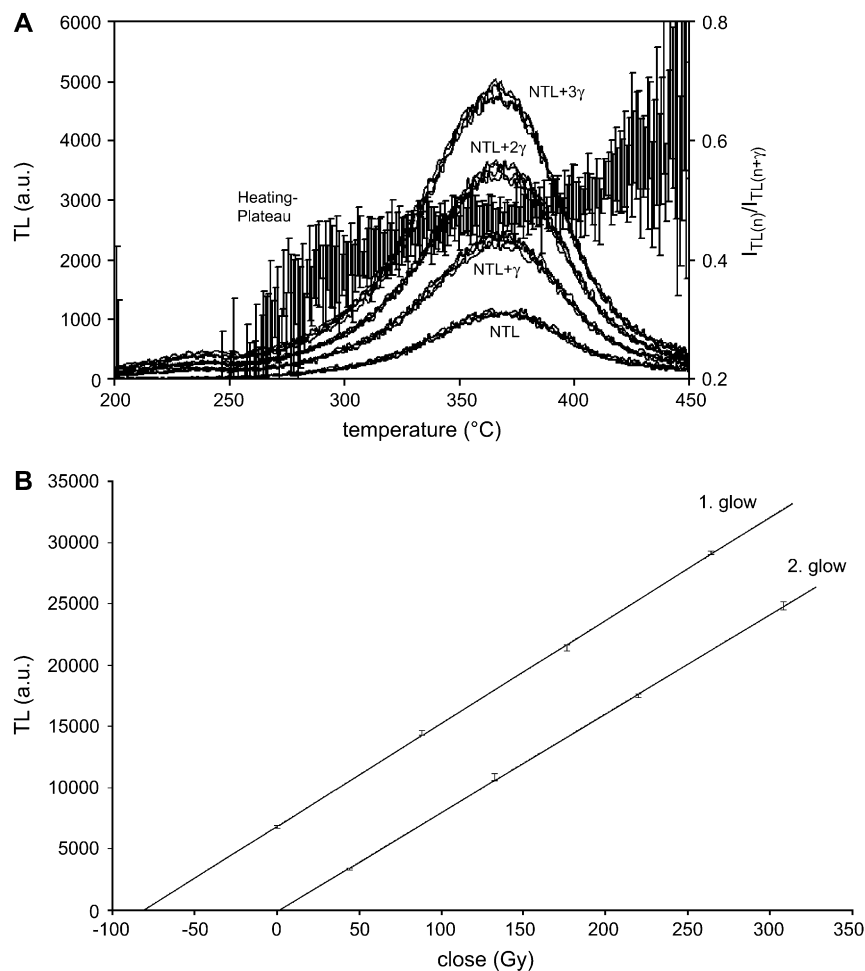


Fig. 4. (A) Natural TL ($I_{\text{TL}(n)}$) and additive TL glow curves ($I_{\text{TL}(n+\gamma)}$, $I_{\text{TL}(n+2\gamma)}$, $I_{\text{TL}(n+3\gamma)}$, $I_{\text{TL}(n+4\gamma)}$) together with the heating plateau ($I_{\text{TL}(n)}/I_{\text{TL}(n+\gamma)}$) of sample BER-13. (B) Additive dose curve (1. glow) for determining the equivalent dose (ED), and regeneration dose curve (2. glow) for the supralinearity correction of sample BER-13.

luminescence of α - and β -irradiated (^{238}Pu and $^{90}\text{Y}/\text{Sr}$, respectively) fine grain discs, employing the S_{α} -system [23].

The variability of S_{α} is large (Table 3), ranging from 11 to $46 \mu\text{Gy}/\text{a}/10^3 \alpha/\text{cm}^2$. These data, again, might reflect the variability of the radioactive element concentrations (see above).

6. Dating results

The resulting ages for Level I range between 54–90 ka and 68–111 ka for Level II. χ^2 analysis shows that neither age distribution is normal. Nevertheless, eight results out of 10 from Level I range from 72 ± 7 (BER-13) to 90 ± 8 ka (BER-17) and are in agreement at one sigma level. The corresponding mean of 80 ± 6 ka falls at the end of OIS 5. The same chronological information is deduced from five of the six ages obtained for the underlying Layer II. With the exception of sample BER-19, which is dated to 111 ± 11 ka, all the results are compatible and range from 67 ± 6 (BER-24) to 88 ± 9 ka (BER-21) with a mean of 75 ± 8 ka. The age reversal for the two levels is apparent, because the results overlap on the one sigma error level. So, it appears that the mean ages obtained for Levels I and II are statistically indistinguishable even though the 1-m thick sterile layer C separates them. The global mean for the two levels (Fig. 5) is 78 ± 7 ka. At present we cannot explain why three samples fall outside the main cluster, as all the TL measurements are coherent, but it has to be suspected that they are intrusive from older and younger archaeological levels. This is supported for the rejected samples BER-10, -14 and -19 by their ratios of palaeodose to internal dose rate (Table 5), which indicate that these samples have been in a different dosimetric environment and are thus of different age.

7. Discussion and conclusion

According to our geological investigations, particularly as regard the extent of soil evolution, the pedogenesis responsible for the composition of Units B and D can be related to OIS 5 but not to the short warm events of OIS 3 (24–59 ka; Ref. [11]). Subsequent to the soil formation these

Table 5
Ratio of palaeodose to internal dose rate data

Lab. N°	BER-	Level	Total internal dose rate ^a ($\mu\text{Gy}/\text{a}$)	Palaeodose (Gy)	Palaeodose/internal dose rate
7		I	378 ± 26	86.7 ± 7.2	0.23
8		I	403 ± 31	84.6 ± 3.3	0.21
10		I	714 ± 58	74.9 ± 3.2	0.10
12		I	364 ± 25	75.8 ± 3.4	0.21
13		I	521 ± 38	84.3 ± 7.0	0.16
14		I	897 ± 66	93.0 ± 3.0	0.10
15		I	492 ± 34	91.2 ± 4.2	0.19
16		I	477 ± 33	91.3 ± 4.3	0.19
17		I	319 ± 22	86.6 ± 4.9	0.27
18		I	505 ± 34	94.0 ± 4.8	0.19
19		II	246 ± 16	142.7 ± 7.8	0.58
20		II	789 ± 61	125.9 ± 6.3	0.16
21		II	937 ± 71	171.6 ± 14.7	0.18
22		II	513 ± 37	116.5 ± 11.5	0.23
23		II	518 ± 41	110.9 ± 4.8	0.21
24		II	482 ± 33	102.6 ± 5.3	0.21

^a Sum of α - and β -dose rates, plus a minor internal γ contribution.

sedimentological units have been disturbed or displaced. Because of their similar appearance and composition they could have been derived from the same origin. Therefore, the temporal relationship of the embedded artefacts to the soil formations cannot be established. However, the effect of the perturbation on the archaeological record was limited. Notably the preservation of the base of a hearth in Unit B provides evidence that the deposition of Unit D (Level II) has to have occurred earlier, and the embedded artefacts thus were deposited prior to the ones from Unit B (Level I). Despite the presence of up to 1-m sterile sediment between these levels, the temporal difference between these depositional events, and consequently the deposition of the artefacts (no matter how they are related to the sediments) remains unclear.

The TL dating results support the attribution of the burnt lithic specimens to the OIS 5 and allow refining the chronology by eliminating the sub-stage 5e. More precisely, the mean of 78 ± 7 ka suggests that the last heating of the lithics of Levels I and II (Units B and D, respectively) took place during OIS 5a (74 – 85 ka). This, however, does not establish the age of the soil reworking on the slope, which is responsible for the present state of these layers. Because Unit C, whose elements have been affected by frost, falls between layers B and D, the soil reworking could have even occurred at the transition from OIS 5 to 4 or even during a cold episode (OIS 4). In the light of the TL-data this cannot be excluded. However, given the dispersion of the TL-data set, an attribution of the lower level (Level II, Unit D) to an earlier OIS 5 sub-stage cannot be entirely ruled out either.

But, the combination of stratigraphic and sedimentological analysis, together with the TL dating results indicate that the assemblages of *Moustérien Ferrassie* recovered from the reworked layers B and D were produced during OIS 5a. Such techno-complexes have also been found at sites such as Artenac (Charente) and Lycée Pons (Charente Maritime), which are attributed to the beginning of the last interglacial – glacial cycle. These lithic industries show affinities with the

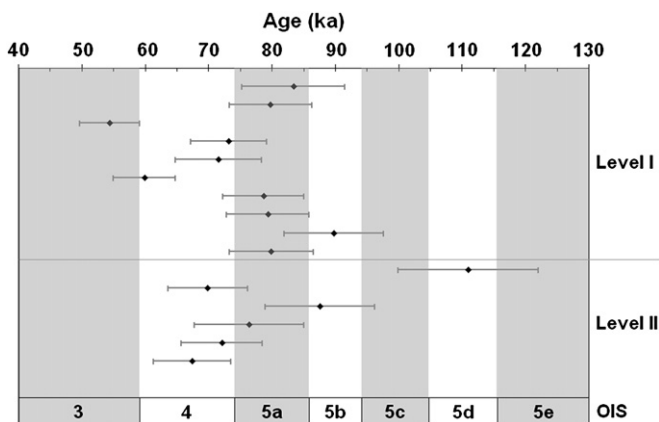


Fig. 5. TL-ages of burnt flints from Berigoule Levels, I and II, in regards of the oceanic isotopic chronology [11]. The errors are given at one sigma level.

Moustérien typique assemblages discovered at Les Canalettes (Aveyron), Baume-Vallée (Haute Loire) and Pié-Lombard (Alpes Maritimes), all three dated to the OIS 5a [6,7,25]. These data indicate that during this period, different techno-complexes (Ferrassie and Typical Mousterian as well as Quina) have been produced in different parts of Southern France.

Acknowledgements

This work was partially funded by the Deutscher Akademischer Austauschdienst (PROCOPE 312-pro-as), by the Minister of Culture (1988–1991), the CNRS and the CEA in France.

References

- [1] M.J. Aitken, Thermoluminescence Dating, Academic Press, London, 1985.
- [2] B.J. Brennan, H.P. Schwarcz, W.J. Rink, Simulation of the radiation field in lumpy environments, *Radiation Measurement* 27 (1997) 299–305.
- [3] J.-P. Brugal, J. Jaubert, P.-J. Texier, Découverte d'un site moustérien de plein-air en Vaucluse, *Bulletin de la Société Préhistoire Française* 86 (1989) 69–71.
- [4] J. Buisson-Catil (Ed.), Le paléolithique moyen en Vaucluse. A la rencontre des chasseurs néandertaliens de Provence nord-occidentale, *Notices d'Archéologie Vauclusienne*, vol. 3, Avignon, 1994.
- [5] J. Jaubert, Murs. Bérigoule, in: J.P. Jacob (Ed.), *Provence-Alpes-Côte d'Azur*, 1990, Gallia Informations, 1990, pp. 272–276.
- [6] J. Jaubert, Chasseurs et artisans du Moustérien, *Maison des Roches-Le Seuil*, Paris, 1999.
- [7] J. Jaubert, Les occupations humaines du Dernier Interglaciaire et de la fin du stade isotopique 5 dans le Sud de la France, in: A. Tuffreau, W. Roebroeks (Eds.), *Le Dernier Interglaciaire et les occupations humaines du Paléolithique moyen*, vol. 8, Publications du CERP, 2002, pp. 143–156.
- [8] J.L. Joron, Contribution à l'analyse par activation neutronique des éléments en traces dans les roches et les minéraux par activation neutronique, Application à la caractérisation d'objets archéologiques, Thèse de 3ème cycle, Université Paris-Sud, 1974.
- [9] S. Lebel, E. Trinkaus, M. Faure, P. Fernandez, C. Guérin, D. Richter, N. Mercier, H. Valladas, G.A. Wagner, Comparative morphology and paleobiology of Middle Pleistocene human remains from Bau de l'Aubésier, Vaucluse, France, *Proceedings of the National Academy of Science of the United States* 98 (2001) 11097–11102.
- [10] H. de Lumley-Woodyear, Le Paléolithique inférieur et moyen du Midi méditerranéen dans son cadre géologique, *Gallia Préhistoire Suppl. V* (1969).
- [11] P.M. Martinson, N.G. Pisias, J.D. Hays, J. Imbrie, T.C. Moore, N.G. Shackleton, Age dating and the orbital theory of the ice ages, development of a high-resolution 0 to 300,000-year old chronostratigraphy, *Quaternary Research* 27 (1987) 1–29.
- [12] N. Mercier, H. Valladas, G. Valladas, Observations on palaeodose determination with burnt flints, *Ancient TL* 10 (1992) 28–32.
- [13] J.R. Prescott, J.T. Hutton, Cosmic ray contributions to dose rates for luminescence and ESR dating: large depths and long-term variations, *Radiation Measurements* 23 (1994) 497–500.
- [14] D. Richter, Thermolumineszenzdatierungen erhitzter Silices aus paläolithischen Fundstellen, Anwendung und methodische Untersuchungen, unpublished Doctoral thesis, University Tübingen, 1998.
- [15] D. Richter, J. Waiblinger, W.J. Rink, G.A. Wagner, Thermoluminescence, electron spin resonance, and ¹⁴C-dating of the Late Middle and Early Upper Palaeolithic site Geissenklösterle Cave in southern Germany, *Journal of Archaeological Science* 27 (2000) 71–89.
- [16] H.P. Schwarcz, Current challenges to ESR dating, *Quaternary Science Reviews* 13 (1994) 601–605.
- [17] P.-J. Texier, Désilicification des silex taillés, *Quaternaria XXIII* (1981) 159–169.
- [18] P.-J. Texier, I. Francisco-Ortega, Main technological and typological characteristics of the lithic assemblages from level 1 at Bérigoule (Murs–Vaucluse), in: H.L. Dibble, O. Bar-Yosef (Eds.), *Monographs in World Archaeology, The Definition and Interpretation of Levallois Technology*, vol. 23, 1995, pp. 213–226.
- [19] P.-J. Texier, J.-P. Brugal, C. Lemorini, L. Wilson, Fonction d'un site de Paléolithique moyen en marge d'un territoire: l'abri de La Combette (Bonnieux, Vaucluse). Économie préhistorique, *Les Comportements de subsistance au Paléolithique*, XVIIIe Rencontres Internationales d'Archéologie et d'Histoire d'Antibes, APDCA, 1998, pp. 325–348.
- [20] G. Valladas, A gamma ray irradiator, *PACT – Revue du Réseau Européen de Sciences et Techniques appliquées au Patrimoine Culturel* 3 (1978) 439–442.
- [21] H. Valladas, Estimation of heating temperature of prehistoric burnt flints by thermoluminescence, *PACT* 9 (1983) 251–253.
- [22] H. Valladas, Thermoluminescence dating of flint, *Quaternary Science Review* 11 (1992) 1–5.
- [23] G. Valladas, H. Valladas, Effet de l'irradiation alpha sur des grains de quartz, *Pact – Revue du Réseau Européen de Sciences et Techniques appliquées au Patrimoine Culturel* 6 (1982) 171–178.
- [24] G. Valladas, N. Mercier, R. Létuvé, A simple semi-automatic TL apparatus of new design, *Ancient TL* 12 (1994) 39–40.
- [25] H. Valladas, N. Mercier, C. Falguères, J.J. Bahain, Contribution des méthodes nucléaires à la chronologie des cultures paléolithiques entre 300,000 et 35,000 ans BP, *Gallia Préhistoire* 41 (1999) 153–166.
- [26] D.W. Zimmerman, Thermoluminescent dating using fine grains from pottery, *Archaeometry* 13 (1971) 29–52.